

# Aerodynamic Drag Reduction of an Automobile

Srinivasa Prasad Katrenipadu  
dept. of mechanical engineering  
JNTUK-UCEV  
Vizianagaram, A.P., India  
ksprasad.me@jntukucev.ac.in

Mani Kumar Velugula  
dept. of mechanical engineering  
JNTUK-UCEV  
Vizianagaram, A.P., India  
velugulamani.me@jntukucev.ac.in

Neelima Devi Chinta  
dept. of mechanical engineering  
JNTUK-UCEV  
Vizianagaram, A.P., India  
cneelima.me@jntukucev.ac.in

**Abstract**— Environmental issues and increased fuel prices are the driving forces for the automotive manufacturers to develop more fuel efficient vehicles with lower emissions. Large investments are aimed at minimizing power needed for propulsion i.e. new downsized engines with aerodynamic devices for drag reduction. For passenger cars, the aerodynamic drag force is the dominating resistance force at higher velocity. The car body is often optimised for reducing the drag resistance. To explain the aerodynamic force in a simplified manner the resisting drag originates from the pressure difference between the stagnation pressure in the front and the base pressure at the rear. By reducing the pressure difference the drag force will be reduced hence the fuel consumption will be reduced.

Aerodynamic drag is one of the main obstacles to accelerate a solid body when it moves in the air. When an automobile or road vehicle burns fuel to accelerate, drag force pulls it from back to reduce the speed and hence the fuel efficiency is adversely affected. About 50 to 60% of total fuel energy is lost only to overcome this adverse aerodynamic force. To get faster acceleration, reducing the drag force by optimizing its shape to ensure stream-lining or reducing the separation is essential. Reduction of aerodynamic drag has become one of the prime concerns in vehicle aerodynamics. This article is concentrated on different aspects analysis of aerodynamic drag of racing cars and different drag reduction techniques such as rake variation and rear under body modification. The drag coefficient of the car is obtained by using AUTODESK FLOW DESIGN and the drag force by ANSYS FLUENT. Car is designed in AUTODESK FUSION 360. It is also evident that if somehow the negative pressure area and its intensity at the rear of the car can be minimized, the separation pressure drag is subsequently reduced.

**Keywords**—aerodynamic drag, automobile, flow separation

## I. INTRODUCTION

### A. Flow separation

As the air travels along the surface of an immersed body the pressure gradient of the boundary layer drops. When the gradient of the velocity profile reaches a value of zero a separation of the flow will occur. As the flow separates the air becomes de - attached from the surface and will instead form eddy. This will result in increased drag or more specifically pressure drag which that a delay in flow separation would have been more favourable in terms of total drag.

## II. DESIGN AND METHODOLOGY

### A. Design

In the current work, various models by modifying the body of the vehicle using the software AUTODESK FUSION

360 are designed. First, the variations are under – body by changing the slicing angle ( $\beta$ ). Various slicing angles are  $0^\circ$ ,  $2.5^\circ$ ,  $5^\circ$ ,  $10^\circ$ ,  $12.5^\circ$  and the designs are as shown from Figure 1 to Figure 5.



Fig. 1.  $\beta = 0^\circ$



Fig. 2.  $\beta = 2.5^\circ$



Fig. 3.  $\beta = 5^\circ$



Fig. 4.  $\beta = 10^\circ$



Fig. 5.  $\beta = 12.5^\circ$

We fixed the slicing angle to  $12.5^\circ$ , we varied the rake of the vehicle as  $15^\circ$ ,  $20.7^\circ$  and  $25^\circ$  as shown from figure 7 to Figure 8.



Fig. 6.  $\beta = 15^\circ$



Fig. 7.  $\beta = 20.7^\circ$



Fig. 8.  $\beta = 25^\circ$

### B. Methodology

First the geometry of the model created in AUTODESK FUSION 360 and is saved in .igs format. Fluid flow (fluent) module is selected from the workbench. The design modeler opens as a new window when the geometry is double clicked. Then go to file and click on the import geometry from external file and then select the .igs format of the model designed in AUTODESK FUSION 360. Now click on generate to display the model. The dimensions of the model are as follows.

- Length of the vehicle = 4000 mm.
- Width of the vehicle = 1500 mm.
- Height of the vehicle = 1200 mm.

We have done this analysis for the model (tool for studying the behaviour of a prototype. It may be smaller, larger or even of the same size as the prototype).

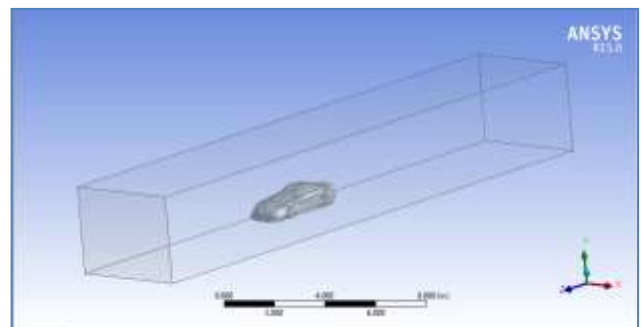


Fig. 9. Geometry model

1) Mesh

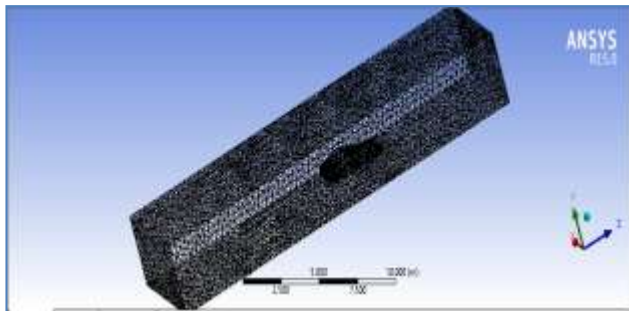


Fig. 10. Meshing model

In free meshing a relatively coarser mesh is generated. It contains both tetrahedral and hexahedral cells having triangular and quadrilateral faces at the boundaries. Later, a refinement of mesh is generated with a refinement of 1.

- The number of nodes generated are 14738.
- The number of elements generated are 67965.

Named selections are given to the solid and fluid domains for which boundary conditions are to be specified for solving the model.

2) Setup and Solution

a) Problem setup

The mesh was checked. The analysis type was changed to Pressure Based type and the velocity formulation was changed to absolute. Time was changed to steady state.

b) Models

Viscous model was selected as k-ε model realizable. The geometry model is shown in Figure 9.

c) Materials

Air as fluid and aluminium as solid was selected from the fluent database by clicking change/create.

- Air – Fluid

Properties given for the air are:

- Density 1.225 kg/m<sup>3</sup> (constant)
- Viscosity 1.7894 x 10<sup>-5</sup> kg/ms (constant)
- Vehicle – Solid (Aluminium)

Properties given for the aluminium are:

- Density 2719 kg/m<sup>3</sup> (constant)

The meshing model is shown in Figure 10.

d) Cell zone conditions

Different parts were assigned as solid or fluid accordingly.

e) Boundary conditions

Different boundary conditions were applied for different zones. The inlet was defined as velocity inlet and outlet was defined as pressure outlet. They are as follows in Table I.

TABLE I. BOUNDARY CONDITIONS

Named section	Boundary condition type	Value
Inlet	Velocity – Inlet	50 m/s
Outlet	Pressure – Outlet	0.0 Pascal

f) Solution methods

The solution methods were set as follows:

- Scheme = Coupled
- Gradient = Least Square Cell Based
- Pressure = Second Order
- Momentum = Second Order Upwind
- Turbulent Kinetic Energy = Second Order Upwind
- Turbulent Dissipation Rate = Second Order Upwind

g) Solution Control and Initialization

Under relaxation factors the parameters are:

- Pressure - 0.75
- Momentum - 0.75
- Density - 1
- Body forces - 1
- Turbulent kinetic energy - 0.8
- Turbulent dissipation rate - 0.8
- Turbulent viscosity - 1

All the conditions were left as default. Then the hot inlet was selected from the compute from drop down list and then the solution was initialized.

h) Convergence criteria

The convergence criteria were set to 10<sup>-5</sup> for the three velocity components and continuity and 10<sup>-14</sup> for turbulent kinetic energy, 10<sup>-20</sup> for turbulent dissipation energy and 10<sup>7</sup> for turbulent viscosity.

i) Run calculation

The number of iterations was set to 1000 with step size 1. Then the calculation was started and it continued till the results converged.

III. RESULTS AND DISCUSSIONS

A. Specimen Results

To get the optimum design of vehicle having less drag coefficient, we compared our model with the standard

vehicle models available. We took some sports models which have less drag coefficient to get faster acceleration and some passenger models which have slightly higher drag coefficients than the sports models. Generally, on an average the drag coefficient of the present day vehicles is of the range 0.2 – 0.3. We analysed the standard models using the software AUTODESK FLOW DESIGN to get their drag coefficients. The model is imported into the software and is kept in a wind tunnel to get the channel of the wind. The standard dimensions of the wind tunnel are as shown in Figure 11.

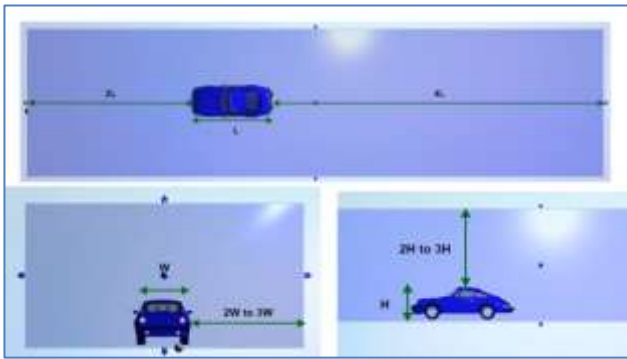


Fig. 11. Wind tunnel dimensions for aerodynamic analysis of a vehicle in AUTODESK FLOW DESIGN software.

Here are some of the standard designs we analysed using AUTODESK FLOW DESIGN to find out the drag coefficients. As discussed earlier, we assumed that the flow to be incompressible and isothermal. By doing this assumption, the density and viscosity of the flow can be seen as constant due to the conditions where the velocity is below Mach number 0.3 ( $Ma = 0.3 \approx 100\text{m/s}$ ). For our analysis, we considered three dimensional flow with air as medium having a velocity 50 m/s according to Indian road conditions.

*a) Sports models*

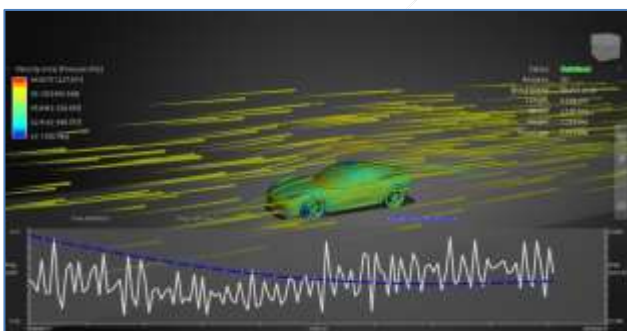


Fig. 12. CHEVROLET C7 CORVETTE – drag coefficient = 0.16

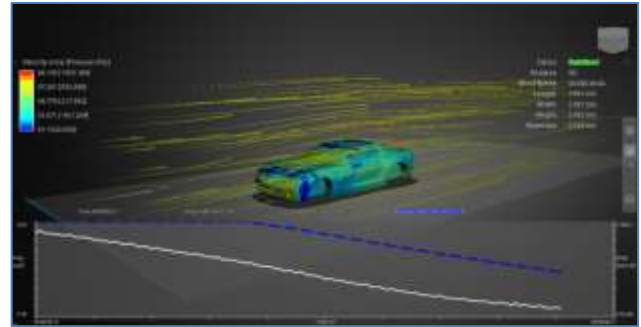


Fig. 13. CHEVROLET C7 CORVETTE – drag coefficient = 0.18

*b) Passenger models*

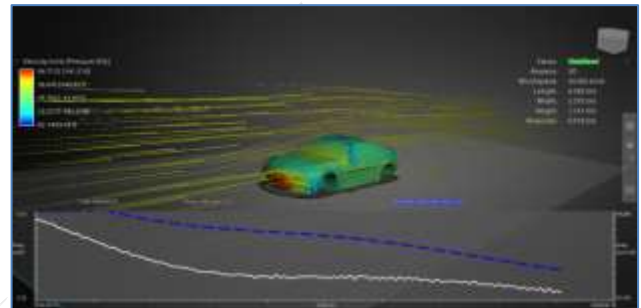


Fig. 14. CHEVROLET C7 CORVETTE – drag coefficient = 0.22

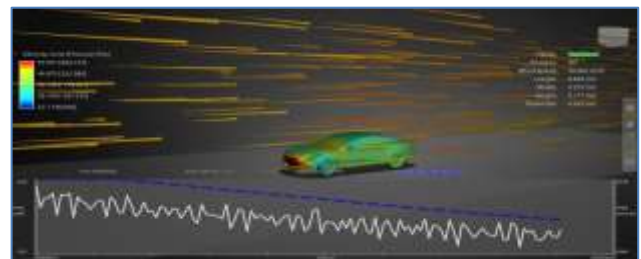


Fig. 15. CHEVROLET C7 CORVETTE – drag coefficient = 0.25

*c) Drag reduction*

When a car moves forward, a low pressure zone is created behind the car. This low pressure zone pulls the car from behind opposite to its moving direction and creates pressure drag. This low pressure zone is created due to the flow separation and consequent vortices are generated at the back of the car. To reduce the pulling – back effect, a unique idea is to slice the rear – body at certain angles as shown from Figure 12 to Figure 15 which eventually directs some flow from under – body to the low pressure zone. This reduces the effect of vortices and low pressure effect. Another way to reduce the rear end separation is to use under –body diffuser as shown in Figure 16 (a), (b) which also adds to the elegance and aesthetics of the car, but it has less flow area as the rear under – body is not fully sliced out. So less reduction of drag is experienced than similar degree of rear under – body slicing. Reduction of drag can also be

achieved by varying the rake of the car. Higher is the rake higher is the separation of the flow and so is the higher pressure drag on the car. By decreasing the rake to an optimum value, we can reduce the drag on the car.



Fig. 16. (a) Rear under – body slicing

(b) Rear diffuser

As the slicing angle increases in case of under body slicing, more air is permitted to flow to the low pressure region. As a result the size of low pressure zone is reduced, this indicates the increase in pressure at that region. So normal force along x axis i.e. the drag force decreases and hence the  $C_d$  decreases too.

**B. Design Results**

The drag results are shown from Figure 17 to Figure 26 and values are tabulated in tables II and III.

*a) Varying slicing angle*

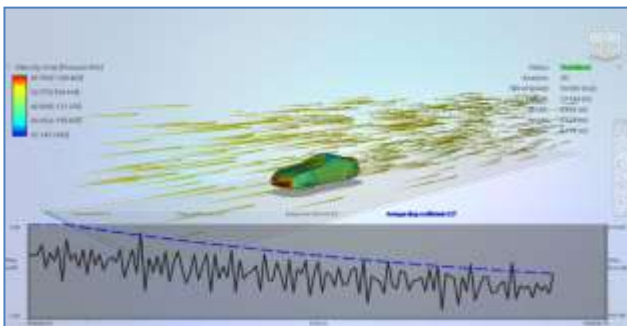


Fig. 17.  $\beta = 0^\circ$ ,  $C_d = 0.29$

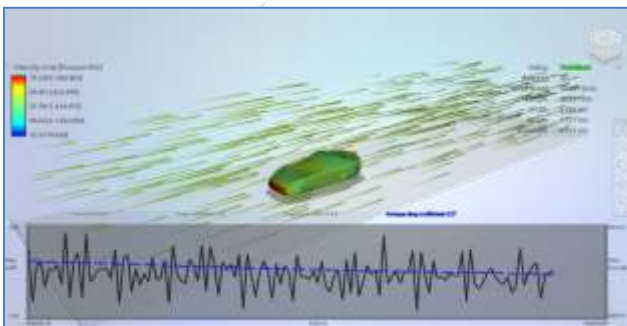


Fig. 18.  $\beta = 2.5^\circ$ ,  $C_d = 0.27$

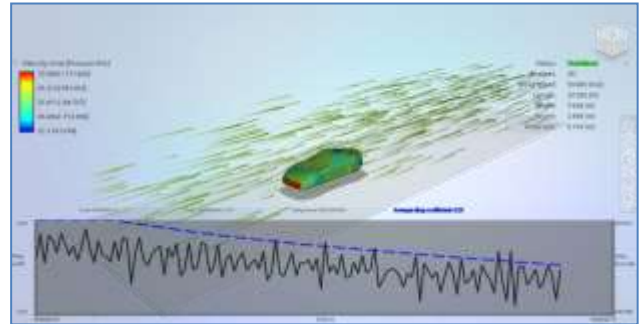


Fig. 19.  $\beta = 5^\circ$ ,  $C_d = 0.26$

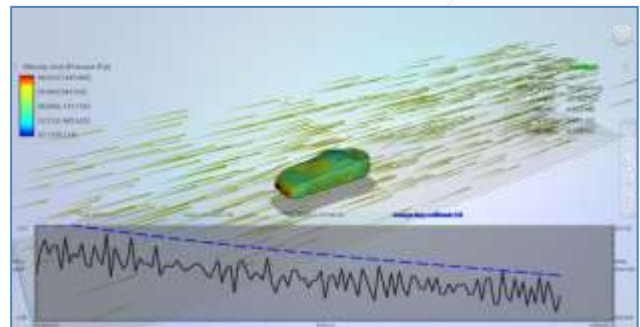


Fig. 20.  $\beta = 10^\circ$ ,  $C_d = 0.24$

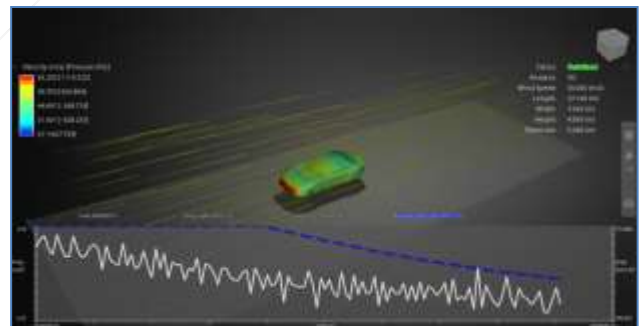


Fig. 21.  $\beta = 12.5^\circ$ ,  $C_d = 0.23$

TABLE II. FOR REAR UNDER- BODY MODIFICATIONS, DRAG REDUCTION AT FLOW VELOCITY 50 M/S

Modification	Description	$C_d$	$\frac{\Delta}{C_d}$	% change
1	$\beta = 0^\circ$	0.29	----	----
2	$\beta = 2.5^\circ$ , rear under – body sliced	0.27	0.09	6.8965517
3	$\beta = 5^\circ$ , rear under – body sliced	0.26	0.03	10.344827
4	$\beta = 10^\circ$ , rear under – body sliced	0.24	0.05	17.241379
5	$\beta = 12.5^\circ$ , rear under – body sliced	0.23	0.06	20.689655
6	$\beta = 15^\circ$ , rear under – body sliced	0.23	0.06	20.689655

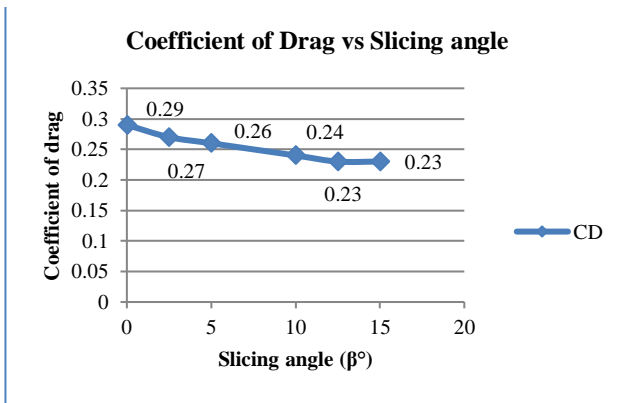


Fig. 22. β = Change in C<sub>d</sub> due to different modification.

b) Varying slicing angle

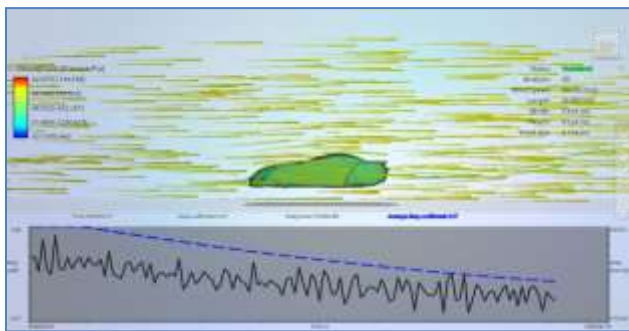


Fig. 23. Rake = 15°, C<sub>d</sub> = 0.27

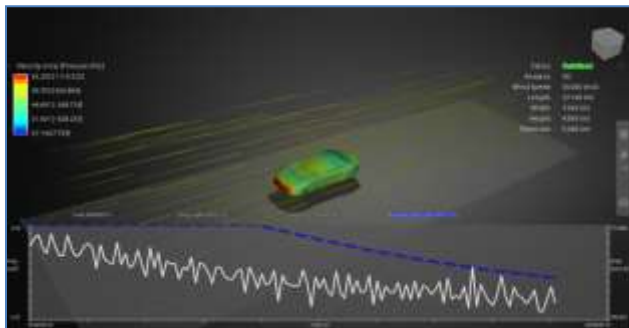


Fig. 24. Rake = 20.7°, C<sub>d</sub> = 0.28

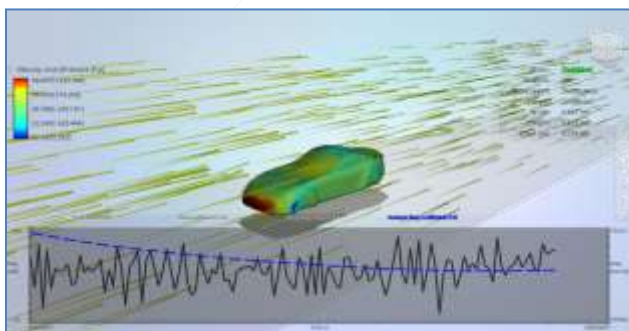


Fig. 25. Rake = 25°, C<sub>d</sub> = 0.29

TABLE III. RAKE VARIATION, CHANGE IN DRAG COEFFICIENT AT FLOW VELOCITY = 50 M/S

Modification	Description	C <sub>d</sub>	$\frac{\Delta C_d}{C_d}$	% change
1	rake = 15°	0.27	---	---
2	rake = 20°	0.28	0.01	3.703703704
3	rake = 25°	0.29	0.02	7.407407407

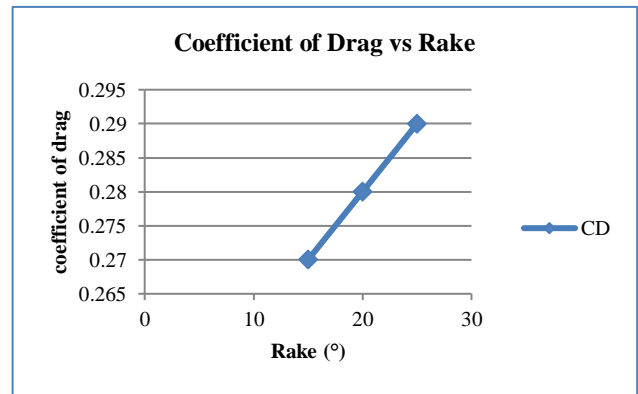


Fig. 26. Change in C<sub>d</sub> due to rake variation

Smaller the amount of rake gives lesser drag coefficient. However when it comes to cabin height, lesser rake become a problem to the passenger. So higher rake are generally adopted in such a way that the drag coefficient is minimum.

c) Results from CFD analysis

The CFD results are shown in Figure 27 and Figure 28.

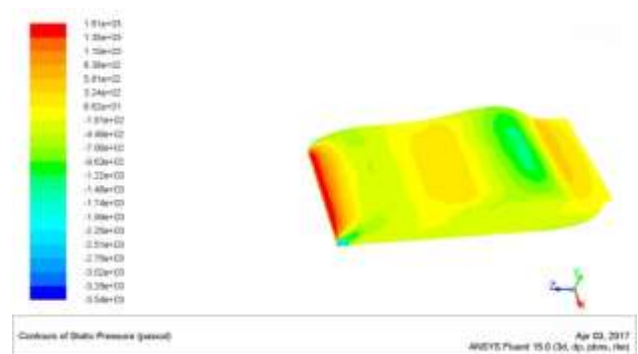


Fig. 27. Static pressure contours on making prescribed design

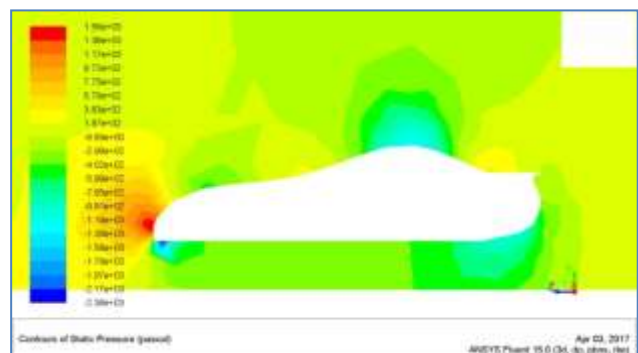


Fig. 28. Static pressure contours at the mid section

#### IV. CONCLUSION

Flow separation is responsible for the major portion of aerodynamic drag of racing cars. The aerodynamic drag coefficient of the car model used here is found to be 0.29. The main design consideration to reduce the drag of any bluff should be- keep the flow attached to the body as much as possible. That means maintaining streamline shape, reducing surface roughness, fewer joints of the body or avoiding sharp fillets, controlling lift force, air flow towards the low pressure zone at the rear portion of the car etc. These must be considered while designing a car for higher speed and acceleration as well as for better fuel efficiency and control. Aerodynamic drag reduction by rear under body modification results in up to 20.6897%.

As the under – body is modified in such a way that the air is made to flow into the region of low pressure zone at the rear side of the vehicle, the pressure drag on the vehicle is decreased thus reducing the drag force and the drag coefficient. As the under – body slicing is increased, the drag coefficient is reduced up to some extent and then increases. The optimum slicing angle for our design is found to be 12.5°.

The drag on the vehicle can also be decreased by varying the rake angle. As the rake angle decreases, the drag coefficient decreases. The optimum rake for our vehicle is found to be 15°. When it comes to the cabin height, lesser rake becomes a problem to the passenger. So higher rake is generally preferred in such a way that the drag coefficient is as minimum as possible.

A model with low drag coefficient of 0.23 with under – body modification of 12.5° slicing angle is obtained.

#### REFERENCES

- [1] Lehueur B., Gilliéron P. & Ivanic T., 2006, "Contribution de l'éclatement tourbillonnaire à la réduction de la traînée des véhicules automobiles: approche numérique", C.R. Mécanique 334 pp. 368-372.
- [2] Krajnovic S. and Davidson L., 2005, "Flow around a simplified car, part 2: Understanding the flow", Journal of Fluid Engineering, 2005, 127, pp. 919-928.
- [3] Gilliéron P. and Chometon F.; "Modelling of stationary three-dimensional detached airflows around an Ahmed Reference Body", Third International Workshop on Vortex, ESAIM, Proceedings, Vol 7, 1999, pp 173-182.
- [4] Chen H., Teixeira C. & Molvig K., 1997, "Digital Physics approach to computational fluid dynamics: some basic theoretical features", Int. J. Modern Phys. C, 8(4), pp. 675-684.
- [5] Rouméas M., Gilliéron P. & Kourta A., 2008, "Separated flows around the rear window of a simplified car geometry", Journal of Fluid Engineering, vol. 130 /021101-1.
- [6] Beaudoin J.F, Cadot O., Aider J.L., Gosse K., Paranthoën P., Hamelin B., 2004, "Cavitation as a complementary tool for automotive aerodynamics, Experiments in Fluids", 37 pp. 763-768
- [7] Spohn A. & Gilliéron P., 2002 "Flow Separations Generated by a Simplified Geometry of an Automotive Vehicle Congrès", IUTAM Symposium on Unsteady Separated Flows, April 8-12, 2002, Toulouse, France
- [8] Fournier G., Bourgois S., Pellerin S, Ta Phuoc L, Tensi J. & El Jabi, R., 2004, "Wall suction influence on the flow around a cylinder in laminar wake configuration by Large Eddy Simulation and experimental approaches", 39e Colloque d'Aérodynamique Appliquée, Contrôle des écoulements, 22-24 Mars, Paris.
- [9] Gilliéron P., 2002, "Contrôle des écoulements appliqués à l'automobile. Etat de l'art", Mécanique & Industries 3, pp 515-524
- [10] Collis, S.S., Joslin R.D., Seifert A., Theofilis V., 2004, "Issues in active flow control: theory, control, simulation, and experiment", Progress in Aerospace Sciences, 40, 237-289.